J Mater Sci (2009) 44:160–165
DOI 10.1007/s10853-008-3102-3

SiC nanofibers by pyrolysis of electrospun preceramic polymers

B. M. Eick · J. P. Youngblood

Received: 29 July 2008 / Accepted: 3 November 2008 / Published online: 27 November 2008
© Springer Science+Business Media, LLC 2008

Abstract Silicon carbide (SiC) nanofibers of diameters as low as 20 nm are reported. The fibers were produced through the electrostatic spinning of the preceramic poly(carbomethylsilane) with pyrolysis to ceramic. A new technique was used where the preceramic was blended with polystyrene and, subsequent to electrospinning, was exposed to UV to crosslink the PS and prevent fiber flowing during pyrolysis. Electrospun SiC fibers were characterized by Fourier transform infrared spectroscopy, thermo gravimetric analysis-differential thermal analysis, scanning electron microscopy, transmission electron microscopy, X-ray diffraction, and electron diffraction. Fibers were shown to be polycrystalline and nanograined with β-SiC 4H polytype being dominant, where commercial methods produce α-SiC 3C. Pyrolysis of the bulk polymer blend to SiC produced α-SiC 15R as the dominant polytype with larger grains showing that electrospinning nanofibers affects resultant crystallinity. Fibers produced were shown to have a core–shell structure of an oxide scale that was variable by pyrolysis conditions.

Introduction

Electrospinning [1, 2] is a technique for producing fibers from the micrometer down to the tens of nanometers scale, whereas conventional spinning produces fibers much larger [3–5]. Electrospinning has been applied to a wide variety of materials and applications such as polymers, biological material [6–8], and ceramics [9–11], with fibers down to 16-nm diameter having been produced [12–15]. In the electrospinning process, an electric field is applied to a polymer solution within a syringe or pipette. When the electrostatic potential overcomes the surface tension of the solution, a tendril jets toward the substrate. Fiber diameter and mat morphology can be controlled using a combination of heating rates, distance to the substrate, and spinning voltage [16]. With a simple plate as the ground electrode, a fibrous mat is formed where the fibers are arranged randomly. Orientation can be attained using a rotating mandrel to wrap the fibers around or by use of a deflection voltage [17].

Although there are many uses for polymeric nanofibers, high temperature or high modulus applications generally require ceramics. Silicon carbide (SiC) is an ideal material for many of these applications such as electronic [18] and optoelectronic applications [19], high-temperature applications [20], solid-state lubricants [19], and harsh environments [21, 22]. The added benefits of using SiC nanofibers in these applications include a requiring lower volume and weight percentage of SiC in a part. The lower amount of SiC would lead to weight and cost savings, and increased efficiency. Electrospinning has been used to prepare ceramic fibers (200–600-nm diameter) by sol–gel processes using hydrophilic polymer fibers as templates [9, 10]. However, this process is slow and limited in ceramic choice to metal oxides [11] and as such non-oxide ceramic nanofibers have been relatively unreported. The production of SiC nanoscale fibers from electrospun templates has been demonstrated by an unwieldy process involving transforming electrospun polyacrylonitrile fibers by repeatedly heating and co-firing with silica (SiO_2) and graphite [23], or carbothermally reducing PVP/TEOS [24] to transform the materials to SiC fibers.

B. M. Eick · J. P. Youngblood (✉)
School of Materials Engineering, Purdue University,
West Lafayette, IN 47907, USA
e-mail: jpyoungb@purdue.edu

Another method to produce non-oxide ceramics is through the use of polymeric precursors, such as poly (carbosilane) [25]. Polymeric preceramics have been of interest for the past few decades. These materials offer the ability to produce materials such as SiC, SiO_2, Si_3N_4, and BN. Melt spinning (and subsequent thermalization) has led to the continuous ceramic fibers such as Nicalon™ and Silyramic™ used in high-performance materials [25–30]. Due to technical considerations of melt-spinning, fibers have been limited to microscale diameters ($\sim$10 μm) [26].

This article presents a method to produce SiC nanofibers by electrospinning of poly(carbomethylsilane) (PCmS) as a ceramic precursor polymer. The SiC nanofibers were produced by a new process where PCmS is blended with polystyrene (PS) to act as an electrospinning aid and to allow post-spinning UV exposure to crosslink the PS and prevent fiber flow and deformation. This method allows for high throughput of fiber production. The polymeric processing methods are faster than traditional ceramic processing methods and the required pyrolysis step required to transform the polymers to ceramics can be carried out at lower temperatures than usual SiC formation temperatures, and in only one step. The authors present diffraction data showing successful conversion to SiC and electron microscopy indicating fiber size and structure.

Experimental

All chemicals were purchased from Sigma–Aldrich (Milwaukee, WI, USA) and used as received. The polymer preceramic, electronic grade PCmS, molecular weight 3500 g/mol solvated in toluene with 5 wt.% dimethylformamide and 5 wt.% tetrabutyl ammonium bromide to increase the electrical conductivity of the solution. PS was added to increase the spinability of the solution at 3 wt.%. The conductive solution was drawn into a glass pipette fitted with a polypropylene tip (7631, Matrix, Hudson, NH) with an opening diameter of 350 μm. The solution was electrospun at ambient temperature, with optimized voltage at 40 kV onto a wire and aluminum foil target at a working distance of 28 cm using a high-voltage DC power supply (SL300, Spellman, Hauppauge, NY). The fibers were collected and placed under a 254-nm wavelength UV lamp for 24 h to crosslink the PS. The fibers were then placed into a tube furnace and pyrolyzed to 1200 °C [as determined by thermo gravimetric analysis-differential thermal analysis (TGA-DTA)] in flowing 5% hydrogen balance argon gas.

Fourier transform infrared spectroscopy (Magna-IR 550, Thermo-Nicolet, Madison, WI) operated in transmittance, TGA-DTA (SDT 2960, TA Instruments, New Castle, DE) operated under flowing nitrogen at 1639 cm^3/min, field emission transmission electron microscopy (FETEM) (80/300 Titan, FEI, Hillsboro, OR) operated at 80 kV accelerating voltage, field emission scanning electron microscopy (FESEM) (S4800, Hitachi, Irvine, CA) operated at 5.0 kV accelerating voltage, transmission electron microscopy (TEM) (JEM-2000FX, JEOL, Tokyo, Japan) operated at 200 kV accelerating voltage, and Cu Kα X-ray diffraction (XRD) (D500, Siemens, Madison, WI) were used to characterize the nanofibers. Electron diffraction (ED) was carried out in the TEM. Fibers were examined as-fired in the TEM, sputter coated with carbon for 60 s before examination in the FETEM, and sputter coated with gold/palladium for 120 s before examination in the FESEM.

Results and discussion

Processing parameterization

Electrospinning of PCmS is not possible due to its short chain length and low-molecular weight. In general, the viscosity of PCmS polymers in solution is not high enough when sheared in the pipette during electrospinning, but this can be overcome with the addition of a higher molecular weight polymer as has been performed before in dry spinning of PCmS [31]. Here, PS is used as it is soluble in a variety of solvents, has a variety of molecular weights available, is vitreous, and contains aromatic groups capable of radiation-induced crosslinking. Upon solvent evaporation, the electrospun fibers will not flow due to vitrification of the PS. However, during pyrolysis, the PS will reach the glass transition temperature before the preceramic polymer sets and the fibers will be prone to deformation. Therefore, after electrospinning fibers were placed under a 254-nm wavelength UV light source to crosslink the PS and add stability to the fibers before the ceramic transition occurs. Addition of the lowest percentage of polymer, while still adding significant viscosity, is important because it prevents voids from forming in the fibers as the PS burns out during pyrolysis.

A systematic study of the PS and PCmS combinations was performed varying molecular weights of PS, ratios of PS to PCMS, and concentration of polymers in solution to develop the optimal formulation, which is presented here. Figure 1 shows the effect of formulation on fiber diameter with each data point representing 20–25 fiber diameters. Generally, an increase in molecular weight of the PS allows less to be used while still attaining good viscosity and fiber production. However, there is a polydispersity of fiber diameters at all concentrations of PS. Increasing the molecular weight of the PS from 280000 to 2000000 g/mol made it possible to decrease the PS in the solution from 15 to 3%. Additionally, it should be mentioned that PS and

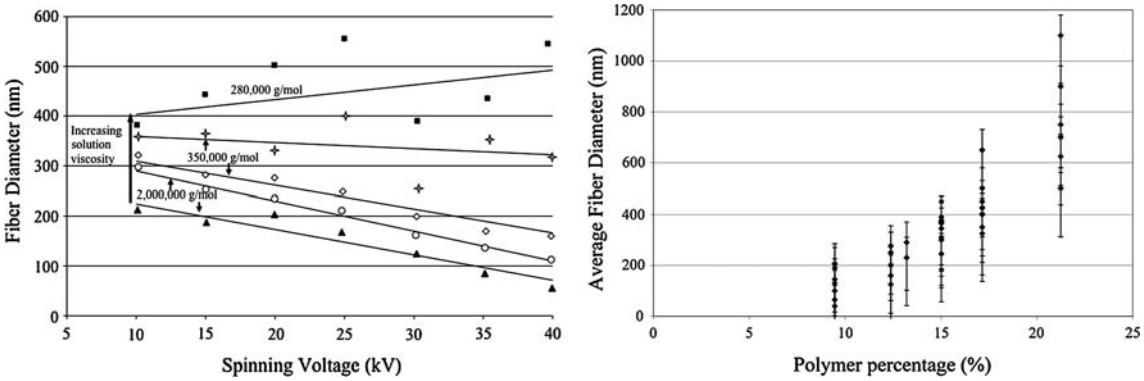

Fig. 1 Process parameter and formulation effects on fiber diameter. Fiber diameter varies as a function of molecular weight and spinning voltage (left) and total polymer loading (right) of PCmS/PS fibers. Manipulation of these parameters allows control of fiber diameter into the nanoscale with a minimum of PS content for 2000000 g/mol molecular weight PS

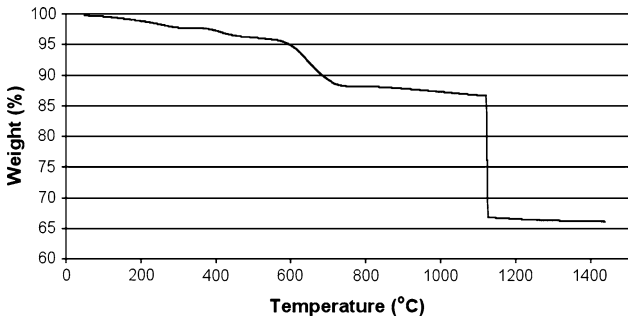

Fig. 2 TGA-DTA weight percent versus temperature profile of preceramic polymer solution as temperature increases from room temperature to 1500 °C, showing the weight loss during the transformation from polymer to ceramic

PCmS are also likely to be incompatible and phase separation is likely upon solvent removal. However, the effect of this incompatibility on the fibers is uncertain.

The heating profile of the pyrolysis step was determined based on experimental data from TGA-DTA run in 5% H_2 balance Argon (same as used in the pyrolysis) at 10 °C/min. TGA-DTA data in Fig. 2 show that the PS burns out at 400 °C, the carbosilane undergoes ceramization starting at 670 °C, and SiC crystallization is observed at ~1175 °C. These transitions are unexceptional and, importantly, the transition at ~1175 °C conforms to previous reports of the PCmS to SiC crystallization [32]. At temperatures higher than 1175 °C, it was found that the fibers begin to break down, possibly due to SiC crystal growth, so 1200 °C was chosen as the pyrolysis temperature for all subsequent fibers.

Electron microscopy

Figure 3 shows a typical FESEM image of the as spun fibers with an average fiber diameter of 50 nm. The preceramic nanofibers were pyrolyzed in nitrogen for 2 h at 1200 °C. FESEM of the resultant fibers is also shown in Fig. 3. The FESEM shows that nanoscale fibers were produced after pyrolysis. During pyrolysis, the PCmS transforms to SiC as in Eq. 1.

$$[\mathrm{MeHSiCH_2}]_n \xrightarrow{1200\,^\circ\mathrm{C}} n\mathrm{SiC} + n\mathrm{H_2} + n\mathrm{CH_4} \quad (1)$$

This process takes place by the PCmS first forming a crosslinked material that then forms an amorphous SiC-type material. At ~1175 °C, crystallization occurs to the final form [32]. The stabilization of the fibers by the addition of PS before firing allows the fibers to keep their shape and morphology after pyrolysis. The beads on the electrospun fibers are expected and are most likely due to the evaporation rate of the solvents used in the system [33].

TEM of the fibers was performed and is shown in Fig. 4. There is little evidence for large-scale voiding in the fibers, however, structure is apparent. While smaller fibers were observed, this fiber is a best result in showing this structure. The lack of voids can be attributed to the low percentage of PS in the electrospinning solution. While it is possible that the fine structure is carbon inclusions and/or grains, measurements do not allow determination of the fine structure. Also apparent are line-like structures at an angle to the fiber in the center of the fiber near the bottom edge that resemble shear bands. Twinning is ruled out as the cause of these structures due to a nanocrystalline grain morphology being smaller than the lines and angles not corresponding to published twin angles of SiC.

X-ray diffraction

XRD spectra (Fig. 5) of the fibers show broad peaks that are indicative of SiC, and do not show a peak indicative of graphite or non-graphitic carbon at 26.6° (although only the >30° spectra are shown due to interference from the amorphous support) [34]. The broad peaks make it difficult to verify the phase and polytype or polytypes of the SiC

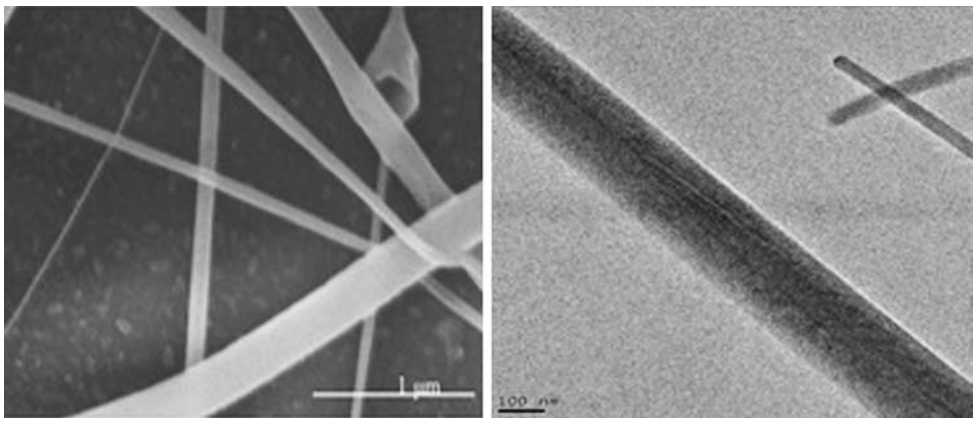

Fig. 3 Representative FESEM micrographs showing the variation in sizes typical of as spun PCmS/PS fibers (left) and pyrolized fibers (right). Both micrographs have fibers above and below 100 nm

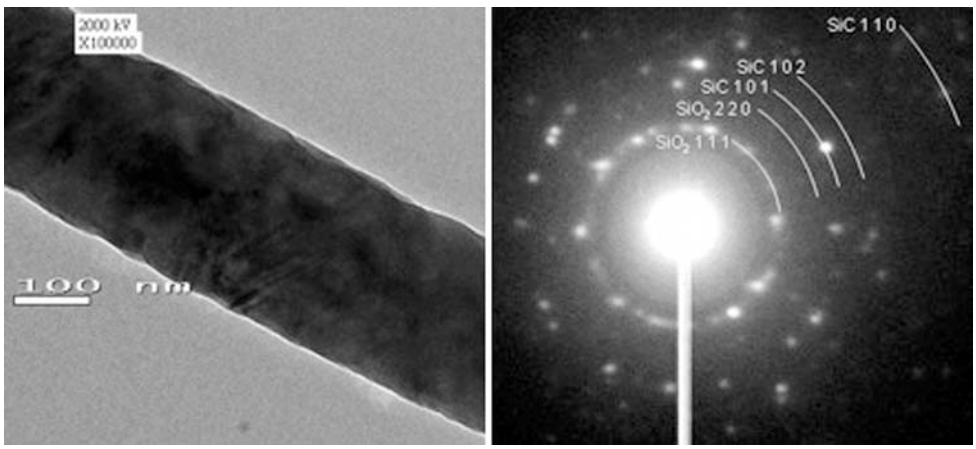

Fig. 4 TEM micrograph of a SiC nanofiber (left) and ED of the fiber (right) showing peaks corresponding to SiC and crystalline silica

produced here and may be due to the nanocrystallinity of the SiC fibers. The nanocrystallinity is not surprising due to the size scale of those fibers as the crystallites must be the same or smaller than the fibers. *As fibers can have nanoscale diameters, by logical extension so must the crystallites*. ED was performed (Fig. 4) and confirmed the presence of both crystalline SiC and crystalline silica and showed that the fibers were polycrystalline. FT-IR was performed and the results agree with XRD and ED that SiC and silica are present (results not shown).

SiC is notoriously difficult to determine the polytype because there are some angles where up to five polytypes share a peak [35]. The peaks and rings here are most closely associated with α-SiC, 4H polytype as shown by the d-spacing given in JCPDS files [36]. Due to the similarities in polytypes, it is possible that multiple polytypes may be represented by some of the fainter peaks. No difference was observed in polytypes by varying electrospinning conditions or size scale. However, regardless of polytype determination of the nanofibers, it is interesting that studies conducted on Nicalon™ fibers derived from PCmS show that grains are *β*-phase SiC, 3C polytype [37].

In order to determine whether or not it is the electrospinning process or other processing parameters such as the material blending that imparts a unique SiC phase or polytype into the material, the preceramic electrospinning solution was pyrolyzed without having been electrospun.

As seen in the XRD spectra in Fig. 5, the material resulting from the preceramic solution, that was not electrospun, was α-phase SiC, 15R polytype. Also, the peaks were sharp and distinguishable, compared with peaks from fibers and must therefore have much larger crystallites than in the fibers. The results of this experiment are just as surprising as that of the fibers. It is possible that the electrospinning process, the thermal processing or the PS/PCmS system that was used, changes the polytype from the expected 3C of the commercial fibers. However, the differences in polytype between electrospun nanofibers and bulk material show that there are effects due to the electrospinning process or the nanofiber morphology that can affect polytype.

The Scherrer equation was applied to the XRD plots to aid in determining the grain size within the electrospun fibers that were crushed and placed in the XRD. The

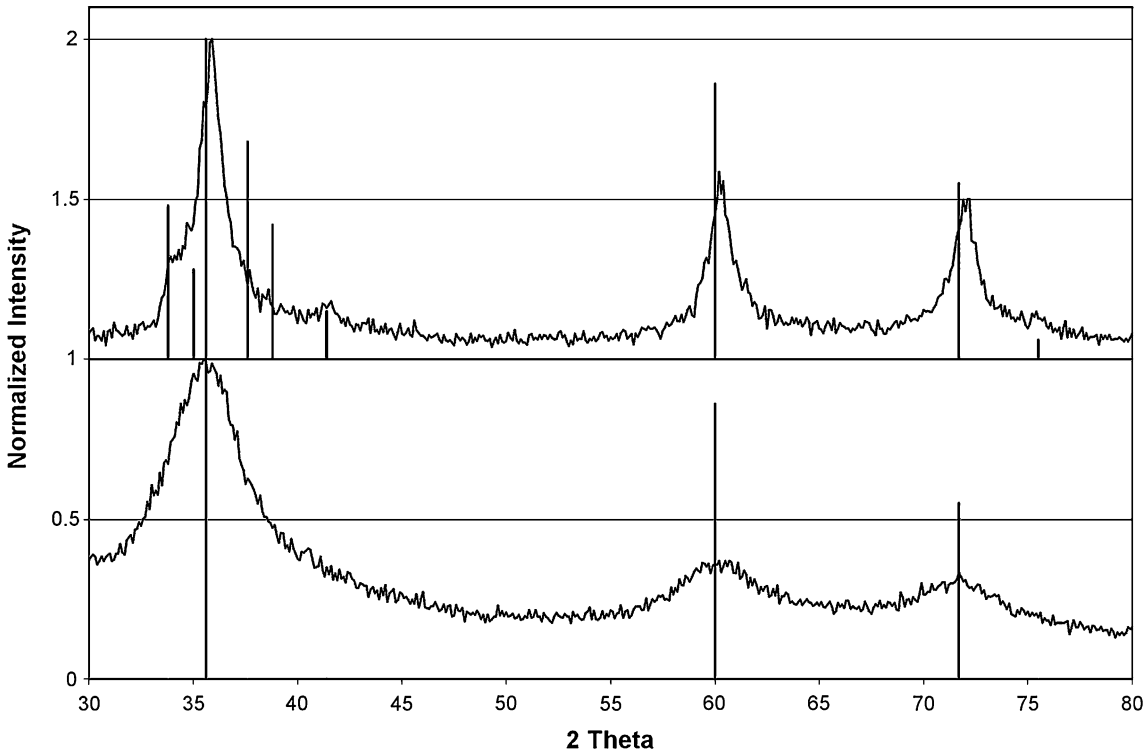

Fig. 5 XRD spectra of SiC precursor solution that was (top) placed directly in the furnace without having been electrospun and (bottom) crushed electrospun fibers after pyrolysis step. Vertical lines correspond to SiC peaks

Scherrer equation uses the breadth of the peak at half of the maximum height of a peak to estimate grain size. It was determined that the electrospun fibers have an average grain diameter of 1.25 ± 0.1 nm while the non-electrospun material was calculated to be 6.1 ± 0.5 nm grain size. However, the Scherrer equation breaks down for materials with multiple polytypes as the peaks may contain shoulders or peaks from multiple polytypes in similar areas. The breakdown of the Scherrer equation explains the anomalously low grain sizes and the discrepancy between the calculated grain sizes and the grain sizes in the TEM micrographs in Figs. 4 and 6. The ED pattern in Fig. 3b also adds credence to the theory that there are multiple polytypes in the fibers due to the fainter rings that are not easily identified as 4H peaks.

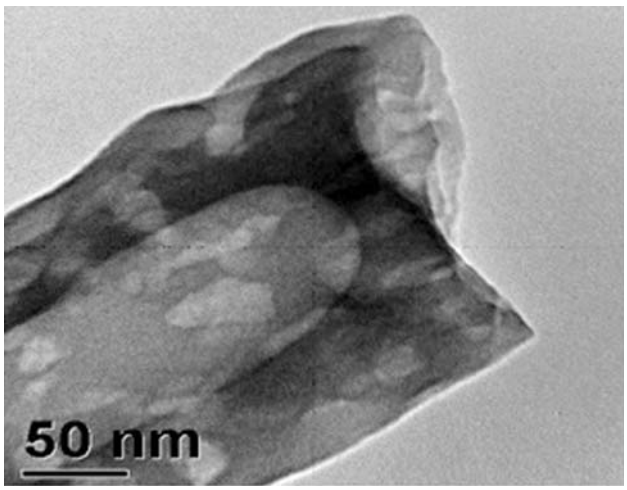

Fig. 6 TEM micrograph of SiC/silica nanofiber showing core/shell structure

Core–shell structure

Further inspection of pyrolyzed fibers in the TEM shows that there is a core–shell structure on the fibers, as seen in Fig. 6. An oxide shell is known to grow on all SiC fibers due to various sources of oxygen such as the room atmosphere, furnace atmosphere, and impurities in the furnace tube [38–40]. Figure 6 shows the core–shell structure of the electrospun SiC fibers. These fibers were shown to be silica and SiC by ED and it is expected that the outer layer is silica. While great care was taken to remove oxygen from the furnace system, even the smallest amount of oxygen would contribute to the formation of a crystalline silica shell. This behavior was not unexpected due to the fast diffusion of oxygen at the nanoscale. In the case of the process here, our fibers had oxide layers with the thinnest attained being 30 nm. In comparison, commercial SiC nanoparticles have a native oxide layer of at least 100 nm [39]. Thus, there is a lower limit to the fiber diameters

produced by this process because of the native oxide layer that forms during processing. If the fiber diameters are smaller than 30 nm, it is likely that the fiber will consist of entirely "shell" with no core. In an effort to limit the oxide layer thickness, it was found that the thickness of the native oxide shell is process parameter dependant and can be adjusted to control the growth of such oxide as presented in Fig. 6. While these studies will not be presented here as this is not the focus of this work, generally, higher temperatures and/or longer temperature treatments result in thicker oxide layers [39, 40].

Conclusions

(1) A new process was developed whereby a polymer preceramic material was electrospun with a high-molecular weight spinning aid (to introduce viscosity) that could undergo post-spinning crosslinking by UV to prevent fiber flowing during thermolysis.
(2) Nanoscale SiC fibers were produced from polymer preceramic materials by pyrolyzing the resultant fibers subsequent to electrospinning process.
(3) TEM, ED, and XRD show that nanofibers were produced as nanocrystalline α-SiC with a silica shell.
(4) Electrospinning, the thermal processing, and/or nanoscale structure seems to impart a different phase and polytype onto the final SiC material from that of non-electrospun material.

Acknowledgements This study was partially supported by the Air Force Office of Scientific Research Grant #F49620-04-NA-153 and the National Science Foundation through the Graduate Assistantship in Areas of National Need. The authors would also like to thank Kent Van Every for help with the FESEM and Prof. Eric Stach with help with TEM.

References

1. Taylor G (1969) Proc R Soc Lond A 313:453
2. Formhals A (1934) US Patent 1975504
3. Deitzel JM, Kleinmeyer J, Harris D, Tan NCB (2001) Polymer 42(1):261
4. Reneker DH, Chun I (1996) Nanotechnology 7(3):216
5. Doshi J, Reneker DH (1995) J Electrostat 35(2–3):151
6. Jiang HL, Hu YQ, Zhao PC, Li Y, Zhu KJ (2006) J Biomed Mater Res B Appl Biomater 79B(1):50
7. Takahashi T, Taniguchi M, Kawai T (2005) Jpn J Appl Phys 2 Lett Exp Lett 44(24–27):L860
8. Fang X, Reneker DH (1997) J Macromol Sci Phys B 36(2):169
9. Choi SS, Lee SG, Im SS, Kim SH, Joo YL (2003) J Mater Sci Lett 22(12):891
10. Caruso RA, Schattka JH, Greiner A (2001) Adv Mater 13(20):1577
11. Li D, Xia YN (2003) Nano Lett 3(4):555
12. Jaeger R, Bergshoef MM, Batlle CMI, Schonherr H, Vancso GJ (1998) Macromol Symp 127:141
13. He X, Zhang X, Zhang C, Zhou X, Zhou A (2001) Compos Sci Technol 61:117
14. Nechanicky MA, Chew KW, Sellinger A, Laine RM (2000) J Eur Ceram Soc 20:441
15. Krauthauser C, Deitzel JM, Wetze ED, O'Brien D (2003) Abstr Pap Am Chem Soc 226:U442
16. Buchko CJ, Chen LC, Shen Y, Martin DC (1999) Polymer 40(26):7397
17. Ayres C, Bowlin GL, Henderson SC, Taylor L, Shultz J, Alexander J, Telemeco TA, Simpson DG (2006) Biomaterials 27(32):5524
18. Saulig-Wenger K, Bechelany M, Cornu D, Epicier T, Chassagneux F, Ferro G, Monteil Y, Miele PJ (2005) Phys IV France 124:99
19. Raman V, Bhatia G, Mishra AK, Bhardwaj S, Sood KN (2006) Mater Lett 60(29–30):3906
20. Chen D, Gilbert CJ, Zhang XF, Ritchie RO (2000) Acta Mater 48(3):659
21. Cheng QM, Interrante LV, Lienhard M, Shen Q, Wu Z (2005) J Euro Ceram Soc 25(2–3):233
22. Jayaseelan DD, Lee WE, Amutharani D, Zhang S, Yoshida K, Kita H (2007) J Am Ceram Soc 90:1603
23. Ye HH, Titchenal N, Gogotsi Y, Ko F (2005) Adv Mater 17(12):1531
24. Li J, Zhang Y, Zhong X, Yang K, Meng J, Cao X (2007) Nanotechnology 18
25. Hasegawa Y, Iimura M, Yajima S (1980) J Mater Sci 15(3):720. doi:10.1007/BF00551739
26. Barham PJ, Keller A (1985) J Mater Sci 20(7):2281. doi:10.1007/BF00556059
27. Laine RM, Babonneau F (1993) Chem Mater 5(3):260
28. Clade J, Seider E, Sporn D (2005) J Eur Ceram Soc 25(2–3):123
29. Yajima S, Hayashi J, Omori M (1975) Chem Lett 9:931
30. Thorne KJ, Johnson SE, Zheng HX, Mackenzie JD, Hawthorne MF (1994) Chem Mater 6(2):110
31. Toreki W, Batich CD, Sacks MD, Saleem M, Choi GJ, Morrone AA (1994) Compos Sci Technol 51:145
32. Odian G (2004) Principles of polymerization, 4th edn. Wiley, Hoboken, NJ, p 174
33. Zuo WW, Zhu MF, Yang W, Yu H, Chen YM, Zhang Y (2005) Polym Eng Sci 45(5):704
34. JCPDS Card File Number 75–2078
35. Sandlin MS (1991) Master of Science. Purdue University, West Lafayette, IN
36. JCPDS Card File Number 29–1127
37. Chiang YM, Smyth IP, Terwilliger CD, Petuskey WT, Eastman JA (1992) Nanostruct Mater 1:235
38. Opila E (1995) J Am Ceram Soc 78(4):1107
39. Mogilevsky P, Boakye EE, Hay RS, Welter J, Kerans RJ (2006) J Am Ceram Soc 89(11):3481
40. Zhu YT, Taylor ST, Stout MG, Butt DP, Lowe TC (1998) J Am Ceram Soc 81(3):655